An H_∞ Design for Dynamic Pricing in the Smart Grid

Wei-Yu Chiu, *Member, IEEE*, Hongjian Sun, *Member, IEEE*, and H. Vincent Poor, *Fellow, IEEE*

***Abstract*—An H_∞ design for dynamic pricing in the smart grid is proposed. This design jointly considers the operation of a distribution network operator and a market operator. In the design, a ratio of the regulated output energy to the disturbance energy is minimized to address the worst-case scenario. Linear matrix inequality approaches are used to formulate the design problem as a convex problem. Fuzzy interpolation techniques are integrated into the design procedure so that nonlinear grid dynamics can be addressed. In contrast with existing designs, the proposed design can yield a more reliable and practical pricing scheme as shown via simulations.**

***Index Terms*—Dynamic pricing, fuzzy systems, LMI approaches, smart grid.**

I. Introduction

The concept of the smart grid has been proposed to address a variety of challenges in the modern power grid, which include efficient energy use, reduction of CO_2, intelligent diagnosis of grid problems, self-healing mechanisms, high penetration of renewable energy sources (RESs) into conventional girds, and dynamic management of the power supply and demand [1]. To some extent, these challenges are related to the underlying energy management systems (EMSs) of the smart grid and, therefore, a large number of studies have been focusing on various methods that can realize smart energy management. Among them, dynamic pricing has been intensively investigated because of the possibility that a power market mechanism can effectively control the power supply and demand between power grids and microgrids with the help of a cost-effective EMS [2]–[4].

Dynamic pricing is basically a mechanism that dynamically adjusts the power price based on, for example, the overall network load, the profits of the supplier, and the social welfare. Ideally, the power users reduce/increase their power consumption at a high/low price [4]–[7] so that a well-designed pricing scheme can help balance the power supply and demand in the grid network. Various pricing schemes have been investigated, e.g., an area control error (ACE) pricing scheme [8]–[10] and a robust pricing scheme [11]. The ACE pricing scheme is modeled by a differential equation in which the rate of change of the price signal is designed to be proportional to the quantity of the imbalanced energy. By employing additional information on individual power demand at microgrids and the total power generation at the power grid, the robust pricing scheme further enhances the ACE scheme for better energy management in the microgrid system. However, these existing market mechanisms do not address how to distribute power from a power grid to multiple microgrids.

To jointly consider power distribution and dynamic price generation in the smart grid, we include a market operator (MO) and a distribution network operator (DNO) [5] in a network of microgrids, a power grid and locally connected RESs. While the RESs contribute to the power supply, they result in a time-varying network. To deal with the time-varying behavior, we propose an adaptive scheme using a gain scheduling technique: the system operation is partitioned into several regions represented by different operating points. The DNO is then designed at different operating points. The equilibrium point of the overall dynamics is evaluated, and auxiliary dynamical equations are introduced based on this equilibrium point. The proposed DNO can distribute the power according the dynamical equations.

Following the DNO design, we adopt an H_∞ design for the MO using fuzzy interpolation techniques. The price signal is generated according to various fuzzy rules in which the consequent parts containing system parameters, i.e., gains. These gains are evaluated so that the H_∞ criterion can be attained: the ratio of imbalanced energy over system disturbances is kept below a prescribed H_∞ attenuation level. These gains can be determined by solving a set of linear matrix inequalities (LMIs), which is convex.

The main contributions of this paper are summarized as follows. Firstly, a gain scheduling approach is proposed to deal with the time-varying behavior of the network of microgrids. Secondly, this paper considers a joint design of the DNO and MO that allows each microgrid to achieve a certain desired level of energy storage. Finally, we propose a new design for the MO, resulting in a more practical and reliable pricing scheme than the design proposed in [11], as shown in our simulations.

The rest of this paper is organized as follows. Section II describes the system model. Our designs for the DNO and MO are proposed in Section III. Simulation results are presented in Section IV. Finally, Section V concludes this paper.

This work was supported in part by the Ministry of Science and Technology of Taiwan under Grant 102-2218-E-155-004-MY3, and in part by the U.S. National Science Foundation under Grant CMMI-1435778. The research leading to these results has received funding from the European Commissions Horizon 2020 Framework Programme (H2020/2014-2020) under grant agreement No. 646470, SmarterEMC2 Project.

W.-Y. Chiu is with the Department of Electrical Engineering and with the Innovation Center for Big Data and Digital Convergence, Yuan Ze University, Taoyuan 32003, Taiwan (email: chiuweiyu@gmail.com).

H. Sun is with the School of Engineering and Computing Science, Durham University, Durham, DH1 3LE, U.K (hongjian.sun@durham.ac.uk).

H. V. Poor is with the Department of Electrical Engineering, Princeton University, Princeton, NJ, 08544 USA (e-mail: poor@princeton.edu).

II. System Model

For clarity, this section is divided into three subsections: Sections II-A, II-B and II-C discuss the functionality of microgrids, the power grid, and the MO and the DNO, respectively.

A. Microgrids

Microgrids (distributed resource island systems) [12] are defined as "subset self sustainable and autonomus of a power system area that is able to operate independently or connected to the network, and other institutions" (WG IEEE1547-4). The definition of microgrid conceives that a microgrid can operate in both connected and island mode, implying that a microgrid possesses storage capabilities. In this study, each microgrid is assumed to have a local energy storage system with the stored energy state $s_n(t)$, $n = 1, 2, ..., N$. To maintain emergency operation, $s_n(t)$ needs to be kept at a positive working level $\tilde{s}_n > 0$. The individual imbalanced energy $e_n(t)$ can be defined as

$$e_n(t) = s_n(t) - \tilde{s}_n. \tag{1}$$

Microgrid n receives power $v_n(t) > 0$ and $p_{g_n}(t) > 0$ from a locally connected RES and the DNO, respectively. The dynamics of the energy storage system can be expressed as

$$\dot{s}_n(t) = \dot{e}_n(t) = p_{g_n}(t) + v_n(t) - p_{d_n}(t) \tag{2}$$

where $p_{d_n}(t) > 0$ represents the power demand. In general, the value of $v_n(t)$ relies on the time-varying weather conditions since RESs, such as solar panels or wind turbines, are often employed.

We consider shiftable loads [3], [13] so that the power demand $p_{d_n}(t)$ in (2) can be adjusted according to the price signal $\lambda(t)$. The power demand dynamics of microgrid n can be expressed as [8], [11]

$$\dot{p}_{d_n}(t) = \frac{1}{\tau_{d_n}} \times \{f_{d_n}(p_{d_n}(t)) - \lambda(t)\} \tag{3}$$

where $\tau_{d_n} > 0$ is a scale factor and $f_{d_n}(p_{d_n}(t))$ represents the marginal benefit for consuming power $p_{d_n}(t)$. For an affine benefit function, we consider

$$f_{d_n}(p_{d_n}(t)) = b_{d_n} + c_{d_n} p_{d_n}(t) \tag{4}$$

where $b_{d_n} > 0$ and $c_{d_n} < 0$ denote the initial consumer's benefit and the consumer's demand elasticity, respectively.

B. Power Grid

Besides the power inputs $v_n(t), n = 1, 2, ..., N$, provided by RESs, the conventional power grid can deliver power to meet the power demand of microgrids in the network. According to the price signal $\lambda(t)$, the dynamics of power generation can be modeled by

$$\dot{p}_g(t) = \frac{1}{\tau_g} \times \{\lambda(t) - f_g(p_g(t)) - \tau_k \sum_{n=1}^{N} e_n(t)\} \tag{5}$$

where $e_n(t)$ is defined in (1), $f_g(p_g(t))$ represents the marginal cost for generating power $p_g(t)$, and $\tau_g > 0$ is a scale factor. The term $\tau_k \sum_{n=1}^{N} e_n(t)$ with $\tau_k > 0$, interpreted as the additional cost for the excess power generation, is included to ensure stability. For an affine marginal cost function, we consider

$$f_g(p_g(t)) = b_g + c_g p_g(t) \tag{6}$$

with $b_g, c_g > 0$.

C. DNO and MO

The DNO distributes the power $p_g(t)$ generated from the power grid to the connected microgrids. Let $p_{g_n}(t)$ denote the power distributed to microgrid n and hence, we have

$$p_g(t) = \sum_{n=1}^{N} p_{g_n}(t). \tag{7}$$

For a one-supplier one-consumer model [11], all generated power is directly distributed to the microgrid and thus there is no need to consider the DNO. However, if more than one consumer is involved and the individual imbalanced energy $e_n(t)$ needs to be minimized, the DNO is needed, as considered in this study.

The MO tries to balance the energy in the network by generating a price signal $\lambda(t) > 0$. The price signal $\lambda(t)$ from the MO is passed to microgrids and the power grid so that the rates of change of power demand and power generation can be adjusted according to (3) and (5), respectively. Meanwhile, information on the distributed power $p_{g_n}(t)$, power demand $p_{d_n}(t)$, and imbalanced energy $e_n(t)$ is transmitted from the DNO and microgrids to the MO, which helps the MO decide the value of $\lambda(t)$.

The overall network dynamics can be expressed by (2), (3), and (5) subjected to (7). The goal is to design the price signal $\lambda(t)$ at the MO and the power $p_{g_n}(t)$ distributed by the DNO such that the value of $|e_n(t)|$ can be as small as possible for $n = 1, 2, ..., N$, or equivalently, the stored energy $s_n(t)$ can achieve the desired energy level $\tilde{s}_n > 0$ as close as possible. The next section presents the proposed design.

III. Proposed DNO and MO Designs

Section III-A presents the proposed DNO, which is further divided into two components, a gain scheduler and a power distribution operator. The MO is designed in Section III-B. Fig. 1 presents the block diagram of the proposed designs.

A. Proposed DNO Design

1) Gain Scheduler: The network dynamics described by (2), (3), and (5) are time-varying because of the power inputs $v_n(t), n = 1, 2, ..., N$, provided by RESs. To facilitate our DNO design, a gain scheduling approach is used [14]. Define $\mathbf{v}(t) = [v_1(t)\ v_2(t)\ ...\ v_N(t)]^T$. The idea we introduce here is to construct a finite set

$$\mathcal{V} = \{\mathbf{v}^{(1)}, \mathbf{v}^{(2)}, ..., \mathbf{v}^{(L)}\} \tag{8}$$

in which each vector can represent $\mathbf{v}(t)$ at a certain operating point. From a statistical perspective, these vectors in (8) can be chosen via a long-term observation.

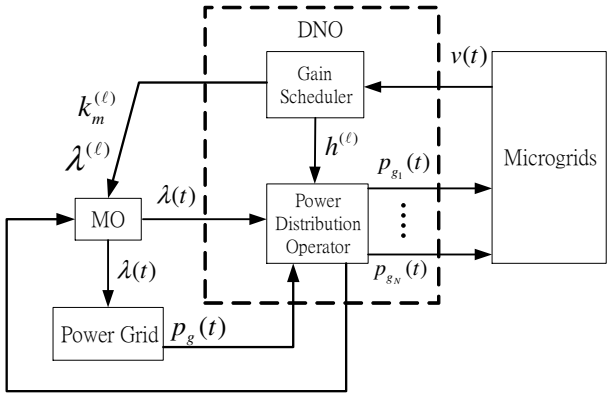

Fig. 1. Block diagram for the proposed DNO and MO.

The set $\mathcal{V}$ is then stored in the DNO, deciding which vector is closest to $\mathbf{v}(t) = [v_1(t)\ v_2(t)\ ...\ v_N(t)]^T$ by

$$\ell = \arg_j \min_{\mathbf{v}^{(j)} \in \mathcal{V}} ||\mathbf{v}(t) - \mathbf{v}^{(j)}|| \tag{9}$$

where $||\cdot||$ denotes the Euclidean norm. In (9), ℓ is a function of time as its value changes according to $\mathbf{v}(t)$, and the error $||\mathbf{v}(t) - \mathbf{v}^{(\ell)}||$ can be reduced by adopting a large L. In control theory, ℓ is referred to as an operating point, and thus we have L operating points according to (8). The gain scheduler performs the operation in (9) so that the MO can use the correct gains $\mathbf{k}_m^{(\ell)}$.

2) Power Distribution Operator: The following theorem derived from using N auxiliary dynamical equations provides a basis for distributing the generated power $p_g(t)$ to the N microgrids.

Theorem 1: Let $p_{g_n}(t)$ be assigned according to

$$\dot{p}_{g_n}(t) = \frac{-c_g}{\tau_g} p_{g_n}(t) - \frac{\tau_k}{\tau_g} e_n(t) - h_n + \frac{1}{\tau_g N}\lambda(t) \tag{10}$$

for $n = 1, 2, ..., N$. Define $e_p(t) = p_g(t) - \sum_{n=1}^{N} p_{g_n}(t)$. For the affine marginal cost function defined in (6), if

$$\sum_{n=1}^{N} h_n = \frac{b_g}{\tau_g} \tag{11}$$

then $e_p(t)$ converges to zero. In particular, (7) is satisfied for all $t \geq 0$ if $e_p(0) = 0$, i.e.,

$$\sum_{n=1}^{N} p_{g_n}(0) = p_g(0). \tag{12}$$

Based on Theorem 1, we can use (10) as the rule of power distribution. The overall network dynamics can then be expressed as

$$\begin{aligned} \dot{p}_{g_n}(t) &= \frac{-c_g}{\tau_g} p_{g_n}(t) - \frac{\tau_k}{\tau_g} e_n(t) - h_n^{(\ell)} + \frac{1}{\tau_g N}\lambda(t) \\ \dot{p}_{d_n}(t) &= \frac{b_{d_n}}{\tau_{d_n}} + \frac{c_{d_n}}{\tau_{d_n}} p_{d_n}(t) - \frac{1}{\tau_{d_n}}\lambda(t) \\ \dot{e}_n(t) &= p_{g_n}(t) + [\mathbf{v}^{(\ell)}]_n - p_{d_n}(t) + [\mathbf{e_v}^{(\ell)}(t)]_n \end{aligned} \tag{13}$$

where $\mathbf{v}^{(\ell)} \in \mathcal{V}$ in (8) and $[\mathbf{e_v}^{(\ell)}(t)]_n = v_n(t) - [\mathbf{v}^{(\ell)}]_n$ for $n = 1, 2, ..., N$. In (13), the superscript "(ℓ)" is used to indicate that the power distribution operator is functioning at operating point ℓ. In Fig. 1, the power distribution operator uses different $\mathbf{h}^{(\ell)} = [h_1^{(\ell)}\ h_2^{(\ell)}, ..., h_N^{(\ell)}]^T$ scheduled by the gain scheduler (9) according to the power input $\mathbf{v}(t)$ provided by RESs.

Let $[(\mathbf{p_g}^{(\ell)})^T\ (\mathbf{p_d}^{(\ell)})^T\ (\mathbf{e}^{(\ell)})^T]^T$ denote the equilibrium point of (13) with $\mathbf{e_v}^{(\ell)}(t) = \mathbf{0}_{N\times 1}$. In light of Theorem 1, $\mathbf{h}^{(\ell)}$ can be chosen such that

$$\begin{aligned} &\left[\ (\mathbf{p_g}^{(\ell)})^T \quad (\mathbf{p_d}^{(\ell)})^T \quad (\mathbf{e}^{(\ell)})^T\ \right]^T \\ &= \left[\ (\mathbf{p_g}^{(\ell)})^T \quad (\mathbf{p_d}^{(\ell)})^T \quad (\mathbf{0}_{N\times 1})^T\ \right]^T \in \mathbb{R}^{3N\times 1} \end{aligned} \tag{14}$$

because it is desirable to have $e_n = 0$ for all n. By combining (13) with (11) and (14), $\mathbf{h}^{(\ell)}$ can be obtained by solving

$$\begin{aligned} &\begin{bmatrix} -\frac{c_g}{\tau_g}\mathbf{I}_N & \mathbf{0}_{N\times N} & -\mathbf{I}_N & \frac{1}{\tau_g N}\mathbf{1}_{N\times 1} \\ \mathbf{0}_{N\times N} & diag(\frac{\mathbf{c_d}}{\tau_\mathbf{d}}) & \mathbf{0}_{N\times N} & -\frac{\mathbf{1}_{N\times 1}}{\tau_\mathbf{d}} \\ \mathbf{I}_N & -\mathbf{I}_N & \mathbf{0}_{N\times N} & \mathbf{0}_{N\times 1} \\ \mathbf{0}_{1\times N} & \mathbf{0}_{1\times N} & \mathbf{1}_{1\times N} & 0 \end{bmatrix} \begin{bmatrix} \mathbf{p_g}^{(\ell)} \\ \mathbf{p_d}^{(\ell)} \\ \mathbf{h}^{(\ell)} \\ \lambda^{(\ell)} \end{bmatrix} \\ &= \left[\ (\mathbf{0}_{N\times 1})^T \quad (-\frac{\mathbf{b_d}}{\tau_\mathbf{d}})^T \quad (-\mathbf{v}^{(\ell)})^T \quad \frac{b_g}{\tau_g}\ \right]^T \in \mathbb{R}^{3N+1}. \end{aligned} \tag{15}$$

In summary, the gain scheduler is operated according to (9), and the power distribution operator performs the power distribution according to (10) with $h_n = h_n^{(\ell)}$ obtained by solving (15). The next subsection presents our MO design based on the established DNO.

B. Proposed MO Design

The purpose of the MO is to generate the price signal $\lambda(t)$ so that the imbalanced energy $e_n(t)$ at microgrids can be driven to zero. Therefore, designing the MO is equivalent to designing the generation of the price signal $\lambda(t)$. To that end, we let $\lambda(t)$ be the control law and minimize the energy of an output vector that consists of $e_n(t), n = 1, 2, ..., N$ as entries.

For convenience, we define

$$\begin{aligned} \mathbf{p_g}(t) &= \left[\ p_{g_1}(t) \quad p_{g_2}(t) \quad ... \quad p_{g_N}(t)\ \right]^T \\ \mathbf{p_d}(t) &= \left[\ p_{d_1}(t) \quad p_{d_2}(t) \quad ... \quad p_{d_N}(t)\ \right]^T \\ \mathbf{e}(t) &= \left[\ e_1(t) \quad e_2(t) \quad ... \quad e_N(t)\ \right]^T \\ \mathbf{x}(t) &= \left[\ \mathbf{p_g}(t)^T \quad \mathbf{p_d}(t)^T \quad \mathbf{e}(t)^T\ \right]^T. \end{aligned} \tag{16}$$

At operating point ℓ, $\lambda(t)$ is designed so that the energy of the output vector

$$\begin{aligned} \mathbf{z}(t) &= \left[\ \mathbf{e}(t)^T \quad \varepsilon(\lambda(t) - \lambda^{(\ell)})\ \right]^T \\ &:= \mathbf{C}\mathbf{x}(t) + \eta\tilde{\lambda}(t) \end{aligned} \tag{17}$$

is minimized, where

$$\mathbf{C} = \begin{bmatrix} \mathbf{0}_{N\times N} & \mathbf{0}_{N\times N} & \mathbf{I}_N \\ \mathbf{0}_{1\times N} & \mathbf{0}_{1\times N} & \mathbf{0}_{1\times N} \end{bmatrix}, \eta = \begin{bmatrix} \mathbf{0}_{N\times 1} \\ \varepsilon \end{bmatrix}, \text{ and } \tilde{\lambda}(t) = \lambda(t) - \lambda^{(\ell)}. \tag{18}$$

In (17), $\tilde{\lambda}(t)$ is multiplied by ε, a control parameter that

controls the tradeoff between the energy management performance and the price signal deviation. Because the difference between $\tilde{\lambda}(t)$ and $\lambda(t)$ is only the constant term $\lambda^{(\ell)}$, we will also call $\tilde{\lambda}(t)$ the price signal. Once $\tilde{\lambda}(t)$ has been generated, $\lambda(t)$ can be immediately recovered by $\lambda(t) = \lambda^{(\ell)} + \tilde{\lambda}(t)$.

Using the DNO proposed in the previous subsection along with the notation defined in (16), the overall network dynamics in (13) can be compactly described as

$$\dot{\mathbf{x}}(t) = \mathbf{A}\mathbf{x}(t) + \mathbf{b}^{(\ell)} + \tau\lambda^{(\ell)} + \tau\tilde{\lambda}(t) + \tilde{\mathbf{e}}_{\mathbf{v}}^{(\ell)}(t) \tag{19}$$

in which

$$\mathbf{A} = \begin{bmatrix} -\frac{c_g}{\tau_g}\mathbf{I}_N & \mathbf{0}_{N\times N} & -\frac{\tau_k}{\tau_g}\mathbf{I}_N \\ \mathbf{0}_{N\times N} & diag(\frac{\mathbf{c_d}}{\tau_\mathbf{d}}) & \mathbf{0}_{N\times N} \\ \mathbf{I}_N & -\mathbf{I}_N & \mathbf{0}_{N\times N} \end{bmatrix},$$
$$\mathbf{b}^{(\ell)} = \begin{bmatrix} -\mathbf{h}^{(\ell)} \\ \frac{\mathbf{b_d}}{\tau_\mathbf{d}} \\ \mathbf{v}^{(\ell)} \end{bmatrix}, \tau = \begin{bmatrix} \frac{1}{\tau_g N}\mathbf{1}_{N\times 1} \\ -\frac{\mathbf{1}_{N\times 1}}{\tau_\mathbf{d}} \\ \mathbf{0}_{N\times 1} \end{bmatrix}, \text{ and} \tag{20}$$
$$\tilde{\mathbf{e}}_{\mathbf{v}}^{(\ell)}(t) = \begin{bmatrix} \mathbf{0}_{N\times 1} \\ \mathbf{0}_{N\times 1} \\ \mathbf{e}_{\mathbf{v}}{}^{(\ell)}(t) \end{bmatrix}.$$

To design $\lambda(t)$ or, equivalently, $\tilde{\lambda}(t)$, we propose to use fuzzy interpolation techniques to interpolate (19). The price signal at the MO can then be designed as

$$\lambda(t) = \lambda^{(\ell)} + \tilde{\lambda}(t) = \lambda^{(\ell)} + \sum_{m=1}^{M} \alpha_m^{(\ell)}(t)(\mathbf{k}_m^{(\ell)})^T\mathbf{x}(t) \tag{21}$$

where $\alpha_m^{(\ell)}(t), m = 1, 2, ..., M$, represent fuzzy bases at operating point ℓ, and $\mathbf{k}_m^{(\ell)}, m = 1, 2, ..., M$, are design parameters that must be determined. By using the LMI approaches introduced in [15], it can be shown that the parameters can be evaluated by solving the LMI constraints described in the following theorem.

Theorem 2: If there exist $\mathbf{Y}^{(\ell)} \in \mathbb{R}^{3N\times 3N}$, $\mathbf{X}_m^{(\ell)} \in \mathbb{R}^{3N\times 3N}$, and $\mathbf{q}_m^{(\ell)} \in \mathbb{R}^{3N\times 1}$ such that (22) at the top of the next page is satisfied, then the H_∞ condition

$$\int \mathbf{z}(t)^T\mathbf{z}(t)dt < (\gamma^{(\ell)})^2 \int \mathbf{w}(t)^T\mathbf{w}(t)dt \tag{23}$$

can be satisfied for the output vector $\mathbf{z}(t)$ in (17) and some disturbance vector $\mathbf{w}(t)$[1]. The gain vectors $\mathbf{k}_m^{(\ell)}$ can be recovered by $\mathbf{k}_m^{(\ell)} = (\mathbf{Y}^{(\ell)})^{-1}\mathbf{q}_m^{(\ell)}$.

IV. Numerical Results

In this section, we describe numerical simulations that have been performed to illustrate our proposed design for the MO and DNO. A network consisting of $N = 3$ microgrids is considered, and Table I lists the parameters used. Suppose that a large L was used, and the set $\mathcal{V}$ defined in (8) was constructed through long-term observation of $\mathbf{v}(t)$. The network dynamics were simulated according to the scenario in which three different operating regions were identified by using (9) during the simulation period:

$$\mathbf{v}(t) \approx \begin{cases} \mathbf{v}^{(1)}, & \text{if } t \in [0, 5], \\ \mathbf{v}^{(2)}, & \text{if } t \in (5, 10] \\ \mathbf{v}^{(3)}, & \text{if } t \in (10, 15] \end{cases}$$

where

$$\mathbf{v}^{(1)} = \begin{bmatrix} 0.09 \\ 2.92 \\ 0.21 \end{bmatrix}, \mathbf{v}^{(2)} = \begin{bmatrix} 3.05 \\ 0.93 \\ 2.39 \end{bmatrix} \text{ and } \mathbf{v}^{(3)} = \begin{bmatrix} 1.24 \\ 1.06 \\ 1.51 \end{bmatrix}. \tag{24}$$

At the DNO with $\mathbf{v}^{(\ell)}$ in (24), the corresponding $\mathbf{h}^{(\ell)}$ and $\lambda^{(\ell)}$ were obtained by solving (15), yielding

$$\mathbf{h}^{(1)} = \begin{bmatrix} 5.48 \\ 3.97 \\ 0.55 \end{bmatrix}, \mathbf{h}^{(2)} = \begin{bmatrix} 9.13 \\ -2.48 \\ 3.36 \end{bmatrix}, \mathbf{h}^{(3)} = \begin{bmatrix} 7.35 \\ -0.21 \\ 2.86 \end{bmatrix}$$
$$\lambda^{(1)} = 7.7037, \lambda^{(2)} = 7.3787, \lambda^{(3)} = 7.6440.$$

Referring to (12) in Theorem 1, the initial conditions

$$p_{g_1}(0) = p_{g_2}(0) = ... = p_{g_N}(0) = \frac{p_g(0)}{N}$$

were chosen, where $p_g(0)$ is the initial condition at the power grid.

Our proposed scheme was compared to the ACE [8] and robust pricing schemes [11] with slight modifications. The robust pricing scheme will be termed the standard scheme as it was derived from a standard LMI design. We examine the numerical results from various perspectives as follows.

A. $\lambda(t)$ at MO

As discussed in [11], the vibration of price plays an important role in managing the imbalanced energy at microgrids. In Fig. 2, the standard and proposed schemes result in prominent price vibration and, therefore, these schemes are expected to

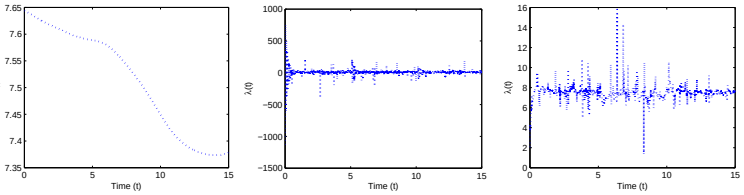

(a) (b) (c)

Fig. 2. Price signal $\lambda(t)$ generated at the MO according to different schemes: (a) ACE scheme with $\lambda(t) \in [7.35, 7.65]$, (b) standard scheme with $\lambda(t) \in [-1500, 1000]$, and (c) proposed scheme with $\lambda(t) \in [1.5, 16]$.

TABLE I
Network Parameters

Microgrids (N=3)	
$\tau_{d_1} = 0.32, \tau_{d_2} = 0.27, \tau_{d_3} = 0.19$	in (3)
$b_{d_1} = 9.11, b_{d_2} = 10.19, b_{d_3} = 11.83$	in (4)
$c_{d_1} = -0.37, c_{d_2} = -0.34, c_{d_3} = -0.65$	in (4)
Power Grid	
$\tau_g = 0.2, \tau_k = 0.1$	in (5)
$b_g = 2, c_g = 0.4$	in (6)

[1]For a matrix $\mathbf{Z}$, $\mathbf{Z} \succ 0$ means $\mathbf{Z}$ is symmetric and positive definite. If $\mathbf{Z} \prec 0$, then it is understood that $-\mathbf{Z} \succ 0$. In (22), the mark "$\star$" is used to denote the terms that can be induced by symmetry. In (23), $\gamma^{(\ell)} > 0$ represents the H_∞ attenuation level.

$$\begin{bmatrix} (-\mathbf{A}_m^{(\ell)}(\mathbf{Y}^{(\ell)})^T - \tau(\mathbf{q}_m^{(\ell)})^T, \star) & -\mathbf{I}_{3N} & \mathbf{X}_m^{(\ell)} + (\mathbf{Y}^{(\ell)})^T - \mathbf{Y}^{(\ell)}(\mathbf{A}_m^{(\ell)})^T - \mathbf{q}_m^{(\ell)}\tau^T & \mathbf{Y}^{(\ell)}\mathbf{C}^T + \mathbf{q}_m^{(\ell)}\eta^T \\ \star & -(\gamma^{(\ell)})^2\mathbf{I}_{3N} & -\mathbf{I}_{3N} & \mathbf{0}_{3N\times(N+1)} \\ \star & \star & (\mathbf{Y}^{(\ell)})^T + \mathbf{Y}^{(\ell)} & \mathbf{0}_{3N\times(N+1)} \\ \star & \star & \star & -\mathbf{I}_{N+1} \end{bmatrix} \prec 0, \quad (22)$$
$$\mathbf{X}_m^{(\ell)} \succ 0, m = 1, 2, ..., M.$$

have better performance of energy management than the ACE scheme. In Fig. 2(b), the standard scheme can produce negative $\lambda(t)$ from time to time. When $\lambda(t)$ is used as an actual market price that must be positive in all instances, such a pricing scheme becomes unrealistic. Furthermore, the standard scheme tends to have a price signal with larger and more intensive vibration than the proposed scheme. By comparing Figs. 2(b) to (c), we conclude that the proposed scheme can adjust $\lambda(t)$ more flexibly than the standard scheme.

B. $p_{g_n}(t)$, $p_{d_n}(t)$ and $v_n(t)$

Because the price signal affects the power distribution and power demand, $p_{g_n}(t)$ and $p_{d_n}(t)$ are expected to change more smoothly in the ACE and proposed schemes than the standard scheme. Fig. 3 provides an overall view on the relation between $p_{g_n}(t)$, $p_{d_n}(t)$ and $v_n(t)$. The standard scheme yields highly vibration in $p_{g_n}(t)$ and $p_{d_n}(t)$ as compared to the other schemes. Furthermore, $p_{g_n}(t)$ and $p_{d_n}(t)$ may assume negative values during the simulation period. For the ACE scheme, the power demand $p_{d_n}(t)$ seems to be insensitive to the changes of $p_{g_n}(t)$ and $v_n(t)$ in comparison with the proposed and standard schemes. In contrast, the proposed scheme presents an excellent pricing scheme as shown in Figs. 3(g)–(i): $p_{g_n}(t)$ increases upon decreasing $v_n(t)$, and decreases when $v_n(t)$ increases; and $p_{d_n}(t)$ responses to the changes of $p_{g_n}(t)$ and $v_n(t)$ to facilitate the process of balancing the energy.

C. $p_g(t)$ at Power Grid and $e_n(t)$ at Microgrids

Fig. 4 shows the power $p_g(t)$ generated at the power grid. Unlike the ACE and proposed schemes, the standard scheme produces both positive and negative values of $p_g(t)$. Although we may interpret a negative value of $p_g(t)$ as power flow from the microgrid back to the power grid, the power flow back and forth between them could be troublesome to the whole power system [16][2].

Finally, the performance of pricing schemes is assessed by the ability to minimize $|e_n(t)|$, which is the main goal of the MO design. In Fig. 5, the proposed and standard pricing schemes, resulting in almost identical performance, outperform the ACE pricing scheme. In summary, the proposed scheme is more appealing among the others: it keeps $p_g(t)$ positive and hence is more practical than the standard scheme; and it achieves better performance of energy management than the ACE scheme.

[2]An LED load was considered and a power factor greater than 0.9 was desired so that most of the energy flows smoothly into the load.

V. Conclusion

A joint design of DNO and MO has been proposed for energy management in microgrid systems. The DNO is designed by introducing auxiliary dynamical equations that mimic the dynamics of power generation at the power grid. The MO is designed by using an H_∞ design together with fuzzy interpolation techniques. The resulting pricing scheme is different from existing schemes: a new LIM formulation for the design of price generation is obtained in comparison with a standard LMI formulation, yielding the capability of adjusting the power generation, power distribution and power demand more smoothly than a standard design.

References

[1] W.-Y. Chiu, "A multiobjective approach to resource management in smart grid," in *Proc. International Conference on Control, Automation and Information Sciences*, Gwangju, South Korea, Dec. 2014, pp. 182–187.

[2] M. Roozbehani, M. Dahleh, and S. Mitter, "Dynamic pricing and stabilization of supply and demand in modern electric power grids," in *Proc. IEEE Int. Conf. Smart Grid Communications*, Gaithersburg, MD, USA, Oct. 2010, pp. 543–548.

[3] H. K. Nguyen, J. B. Song, and Z. Han, "Demand side management to reduce peak-to-average ratio using game theory in smart grid," in *Proc. IEEE Int. Conf. Computer Communications Workshops*, Orlando, FL, USA, Mar. 2012, pp. 91–96.

[4] W.-Y. Chiu, H. Sun, and H. V. Poor, "Demand-side energy storage system management in smart grid," in *Proc. IEEE Int. Conf. Smart Grid Communications*, Tainan City, Taiwan, Nov. 2012, pp. 73–78.

[5] A. L. Dimeas and N. D. Hatziargyriou, "Operation of a multiagent system for microgrid control," *IEEE Trans. Power Syst.*, vol. 20, no. 3, pp. 1447–1455, Aug. 2005.

[6] Z. Zhou, F. Zhao, and J. Wang, "Agent-based electricity market simulation with demand response from commercial buildings," *IEEE Trans. Smart Grid*, vol. 2, no. 4, pp. 580–588, Dec. 2011.

[7] A. Kiani and A. Annaswamy, "Wholesale energy market in a smart grid: Dynamic modeling and stability," in *Proc. IEEE Conf. Decision and Control and European Control Conference*, Orlando, FL, USA, Dec. 2011, pp. 2202–2207.

[8] F. L. Alvarado, "The dynamics of power system markets," Dept. Elect. Comput. Eng., Univ. Wisconsin, Madison, WI, Tech. Rep. PSERC-91-01, Mar. 1997.

[9] A. Kiani and A. Annaswamy, "The effect of a smart meter on congestion and stability in a power market," in *Proc. IEEE Conf. Decision and Control*, Atlanta, GA, USA, Dec. 2010, pp. 194–199.

[10] J. Nutaro and V. Protopopescu, "The impact of market clearing time and price signal delay on the stability of electric power markets," *IEEE Trans. Power Syst.*, vol. 24, no. 3, pp. 1337–1345, Aug. 2009.

[11] W.-Y. Chiu, H. Sun, and H. V. Poor, "Energy imbalance management using a robust pricing scheme," *IEEE Trans. Smart Grid*, vol. 4, no. 2, pp. 896–904, Jun. 2013.

[12] "IEEE guide for design, operation, and integration of distributed resource island systems with electric power systems," *IEEE Std 1547.4*, pp. 1–54, 2011.

[13] M. Roozbehani, A. Faghih, M. I. Ohannessian, and M. A. Dahleh, "The intertemporal utility of demand and price elasticity of consumption in power grids with shiftable loads," in *Proc. IEEE Conf. Decision and Control and European Control Conference*, Orlando, FL, USA, Dec. 2011, pp. 1539–1544.

[14] P. A. Ioannou and J. Sun, *Robust Adaptive Control*. Upper Saddle River, NJ: PTR Prentice-Hall, 1995.

[15] S. Boyd, L. E. Ghaoui, E. Feron, and V. Balakrishnan, *Linear Matrix Inequalities in System and Control Theory*. Philadelphia, PA: SIAM, 1994.

[16] B. Weir, "Driving the 21st century's lights," *IEEE Spectr.*, vol. 49, no. 3 (NA), pp. 42–47, Mar. 2012.

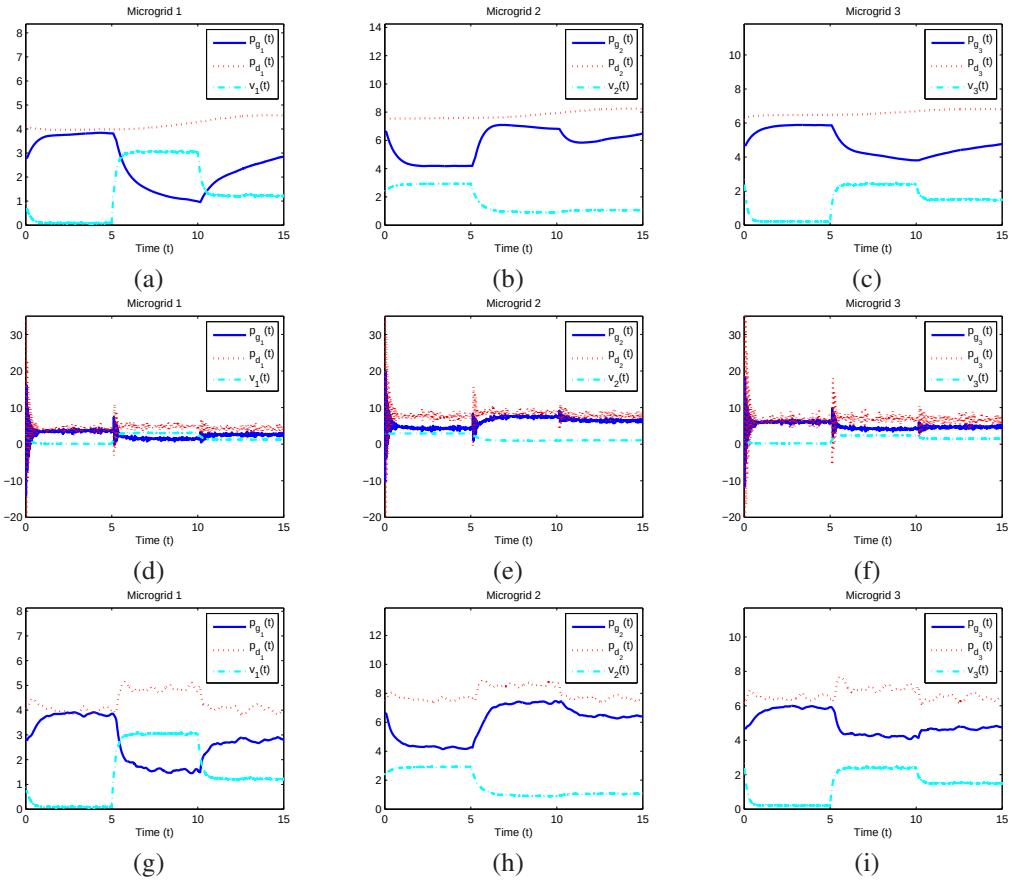

Fig. 3. Relationships among the distributed power $p_{g_n}(t)$, power demand $p_{d_n}(t)$, and power input $v_n(t)$ provided by RESs. Three pricing schemes are compared: (a)–(c) ACE scheme, (d)–(f) standard scheme, and (g)–(i) proposed scheme.

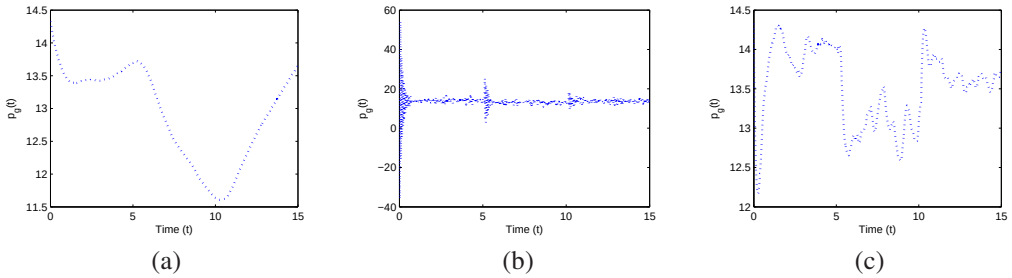

Fig. 4. Power generation $p_g(t) = \sum_{n=1}^{N} p_{g_n}(t)$ at the power grid, where $p_g(t)$ is generated by (a) ACE scheme, (b) standard scheme, and (c) proposed scheme. Unlike the standard scheme in (b), the ACE scheme in (a) and the proposed scheme in (c) can keep $p_g(t) > 0$ for all t.

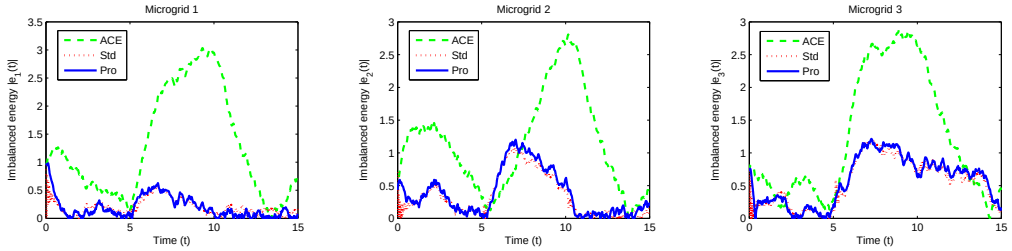

(a) (b) (c)

Fig. 5. Absolute value of imbalanced energy, $|e_n(t)|$, at each microgrid. "ACE", "Std" and "Pro" in the legends represent the ACE, standard and proposed pricing schemes, respectively. A smaller value of $|e_n(t)|$ resulting from a particular pricing scheme means better performance of the corresponding MO. (a), (b) and (c) show the resulting $|e_n(t)|$ at microgrids 1,2, and 3, respectively. The proposed and standard schemes yield almost identical performance for energy management, and they outperform the ACE scheme.